


## Article

# Assessment of the Continuous Extreme Drought Events in Namibia during the Last Decade

Xuan Liu and Jie Zhou \* 

Key Laboratory for Geographical Process Analysis & Simulation of Hubei Province, College of Urban and Environmental Sciences, Central China Normal University, Wuhan 430079, China; liuxuan97@mails.cnu.edu.cn  
\* Correspondence: zhou.j@mail.cnu.edu.cn

**Abstract:** In the context of climate change, the intensity, frequency, and duration of drought events have increased significantly, resulting in a profound impact on both natural ecosystems and socio-economic systems. In arid and semi-arid regions, precipitation is the main limiting factor for vegetation growth, and the ecosystems are very sensitive to climate change. Over the past 10 years, the Namibian government has declared national emergencies in 2013, 2016, and 2019 due to extreme drought events. The continued extreme drought has posed serious threat to the country's food security. Accurately monitoring the continuous drought events in Namibia and assessing their impact on the ecosystem is essential for drought risk management in the region. Based on long-term satellite observation of vegetation index and precipitation, we have evaluated the spatiotemporal dynamics of the three drought events, the vegetation–precipitation relationship across biomes, and the impact of continuous drought events on regional ecosystems. The results suggest that: (1) According to affected area and severity, the drought in 2019 was the most severe one, followed by the drought in 2013; the 2015–2016 drought spread over smaller spatial area, although it continued for two years; (2) Both the accumulated NDVI and precipitation in the growing season in Namibia increased from 2001 to 2010 while showing a significant decreasing trend during 2011–2020; (3) In Namibia, there is a significant correlation between the current season's accumulated precipitation and the current season's accumulated NDVI ( $r = 0.90, p < 0.01$ ). The current season's accumulated precipitation is also well correlated with the next season's accumulated NDVI ( $r = 0.87, p < 0.01$ ), and the correlation between the current season's accumulated precipitation and the next season's accumulated NDVI in a wet year is even stronger ( $r = 0.96, p < 0.01$ ). This indicates that part of the precipitation in the current season may be stored in the soil for the next season's plant growth, which is more obvious in the northern plains with deep-rooted woody plants; (4) In 2013, the drought event suddenly changed from a long-term relatively humid state to an extremely dry state. During the ecological recovery stage, the NDVI during the growing season could not return to the state before the drought, causing irreversible damage to the Namibian ecosystem. In summary, the continuous extreme drought events during the last decade have caused profound impacts on the regional ecosystem. Much more attention should be paid to whether the extreme drought events will continue into the next decade and how the ecosystem can sustain a new equilibrium under a warmer and drier climate.

**Keywords:** vegetation index; precipitation; continuous drought events; ecosystem response; Namibia



**Citation:** Liu, X.; Zhou, J. Assessment of the Continuous Extreme Drought Events in Namibia during the Last Decade. *Water* **2021**, *13*, 2942. <https://doi.org/10.3390/w13202942>

Academic Editors: Yared Bayissa, Assefa M. Melesse and Tsegaye Tadesse

Received: 13 September 2021  
Accepted: 16 October 2021  
Published: 19 October 2021

**Publisher's Note:** MDPI stays neutral with regard to jurisdictional claims in published maps and institutional affiliations.



**Copyright:** © 2021 by the authors. Licensee MDPI, Basel, Switzerland. This article is an open access article distributed under the terms and conditions of the Creative Commons Attribution (CC BY) license (<https://creativecommons.org/licenses/by/4.0/>).

## 1. Introduction

Drought is a creeping phenomenon caused by prolonged water shortage in which the water supply cannot fulfill the requirements of water demand from different sectors, which may result in profound impacts on the ecosystem, agriculture, and livelihoods [1]. According to the basic disciplinary perspective, drought is further subdivided into meteorological drought, agricultural drought, hydrological drought, and socio-economic drought. Drought has long been the world's costliest natural disaster, and most countries experience

serious threat from drought. For example, about 40 million people in southern Africa were affected by drought in the early to mid-1980s, with more than 500,000 deaths [2]. The 1988 drought in the United States caused nearly USD 40 billion in damage, and was the worst natural disaster in U.S. history [3]. The 1991–1992 drought in southern Africa affected about 20 million people and caused a shortage of more than 6.7 million tons of grain supplies [2].

Namibia is one of the sub-Saharan Africa's most arid countries, and also one of the most arid countries in the world [4]. According to the United Nations Development Program (UNDP), the country has experienced recurrent droughts [5]. Namibia experienced severe drought events in the early 1990s and 2000s as well as a perennial drought from 2013 to 2016 [6–11]. In 1992/1993, Southern Africa suffered from a drought that affected the survival of a large part of the population. In Namibia, the severity of the food crisis was sufficiently serious to provoke a massive Drought Relief Program [6,12]. The drought event that occurred in Namibia in 2012/2013 started mainly due to insufficient rainfall. About 300,000 people in the country were affected by the drought and more than 4000 livestock died [13,14]. In 2014/2015 and 2015/2016, Southern Africa experienced an El Niño-induced drought which affected more than 20 countries, including Namibia, with 38 million people exposed to drought across the country [15–17]. Namibia declared a national emergency in July 2016 due to drought. In 2019, the number of people affected by severe drought in sub-Saharan Africa increased to 45 million. Windhoek recorded the lowest rainfall in 2019 since 1891 and Namibia recorded its lowest rainfall in 90 years. More than 500,000 people in Namibia have been affected by the drought, more than 60,000 livestock have died, and locals are facing food insecurity and water shortages [18,19]. The country is frequently impacted by climatic extremes, and droughts threaten millions of people, plants and livestock, leading to water scarcity and food insecurity.

The ecosystems on earth are suffering from the effects of both climate change and human activity, and more frequent and intensive drought events are expected to occur across biomes in the future, which in turn will have a profound impact on natural ecosystems and socio-economic systems [20,21]. There is a correlation between the continuous occurrence of drought events and the decline of ecosystem functions [22–26]. Frequent or intense drought events may change the structure of ecosystems. The severe droughts in the Sahel region of Africa in the 1970s and 1980s caused devastating damage to the regional ecosystem. Thanks to the widespread concern of the international community and residents about environmental issues, rich studies focused on monitoring, assessment and prediction of droughts have been conducted, and adaptation strategies and measures for future climate change have been proposed. Both ground and satellite based evidence suggests that the ecological and environmental conditions seem to be starting to recover in recent years [27,28]. In this case, drought monitoring and assessment are quite important for ecosystem risk assessment.

To accurately monitor the drought dynamic, dozens of drought monitoring indices have been developed based on either ground or satellite observations. A forerunner of drought indicators, the Palmer Drought Severity Index (PDSI), is defined based on soil water balance with clear physical meanings and has been widely used in agricultural drought monitoring; it is always provided as the benchmark for other drought indicators [29]. The Standardized Precipitation Index (SPI) is a precipitation anomaly index defined by comparing current precipitation to long-term (>30 years) local precipitation statistics [30]. Compared to PDSI, which requires precipitation, temperature and soil information as inputs, SPI relies on only precipitation. Additionally, SPI can characterize drought dynamic multiple time scales. It has been recommended by the World Meteorological Organization (WMO) as an index for monitoring widespread meteorological drought [31]. In response to inadequate processes for characterizing agricultural drought, the Standardized Precipitation Evapotranspiration Index (SPEI) was proposed; it considers both water supply (by precipitation) and water demand (by potential evapotranspiration), calculated similarly to SPI. In recent years, SPEI has been widely used in agricultural and ecological drought monitoring and assessment [32]. Traditional drought indices are mostly

defined and calculated based on in situ observation, and the accuracy and reliability of the indices depends more on density of regional ground stations. In undeveloped countries like Namibia, reliable long-term in situ meteorological observations are difficult to assess. In recent years, large-scale and high-frequency remote sensing observations have gradually become the dominant methods for large-scale drought monitoring [33]. Satellite based earth observation sensors such as Advanced Very High Resolution Radiometer (AVHRR), Moderate Resolution Imaging Spectroradiometer (MODIS) and Visible Infrared Imaging Radiometer Suite (VIIRS) have acquired a large amount of multispectral observation that can characterize the global land surface ecosystem dynamics over the past 40 years. Satellite observation-based drought indices such as Vegetation Condition Index (VCI), Temperature Condition Index (TCI), and the Vegetation Health Index (VHI) which integrate vegetation status and canopy temperature have been widely used in drought monitoring and evaluation applications on both regional and global scales since the 1980s [34,35].

In arid and semi-arid regions where precipitation is a major limiting factor for ecosystems, vegetation is greatly sensitive to climate change, and abnormal changes in precipitation during the growing season can further exacerbate the occurrence of drought [36,37]. Precipitation is one of the key links in the water cycle and is also the main source of water for agriculture and animal husbandry in arid regions [38]. Changes in rainfall, rainfall intensity, and rainfall patterns may have serious impacts on agriculture and animal husbandry in arid areas, which in turn may lead to a significant downward trend in productivity and yield [39]. Climate projections indicate that dryness will increase in most arid regions on earth, which may further increase the extent of drought and aggravate land degradation in arid regions [40]. Namibia is an arid and semi-arid country with unstable precipitation patterns. Global climate change may exacerbate abnormal changes in precipitation, leading to frequent extreme events such as floods, persistent droughts, and land degradation, which will have serious impacts on Namibia's ecosystems and further reduce its ability to adapt to climate change [18,41].

Although the extreme drought events occurring in Namibia during the last decade gained broad international attention, few published studies evaluated these events in detail, with the response largely limited to policy and social impacts. For example, Rensburg et al. (2021) assessed the 2015–2017 drought in Windhoek from the perspective of drought management and governance, and Shikangalah et al. (2020) reviewed the 2019 drought in Namibia according to news reports [17,18]. To date, no published studies have investigated the spatiotemporal dynamics of these continuous drought events, and no systematic comparison between the three drought events has been made. To fill this gap, this study aims to evaluate the dynamic of the continuous drought events using freely available observations of rainfall and vegetation, and to assess the impact of long-lasting dry periods on regional ecosystems and livelihoods.

## 2. Materials and Methods

### 2.1. Study Area

Namibia is located in the southwest of the African continent, bordered by Angola and Zambia to the north, Botswana to the east and South Africa to the south (Figure 1a). Namibia covers an area of 825,615 km<sup>2</sup> and is located between the Namib Desert and the Kalahari Desert. The climate in Namibia is hot and dry, with an average annual temperature of 18–22 °C. The four seasons here are spring (September to November), summer (December to February), autumn (March to May), and winter (June to August). With an average annual rainfall of about 250 mm, Namibia is the driest country in sub-Saharan Africa. From Southwest to Northeast, annual average rainfall varies from less than 100 mm in the ultra-arid coastal plain to more than 500 mm in the semi-humid area. Rainfall in Namibia is highly seasonal, with the light rainy season occurring between September and November and the heavy rainy season between February and April. In wetter areas, the rainy season lasts from October to April, but in drier areas, the rainy season starts later and is shorter. The altitude of Namibia is between 1000–2000 m; most of the country is

at an altitude of 1000–1500 m (Figure 1e). The western coastal and eastern inland areas are deserts, the northern part is plains, and the central part is the central highland. The main land cover types are shrubs, grasslands and bare land. Precipitation distribution and vegetation cover distribution in Namibia are spatially consistent, showing a decreasing trend from northeast to southwest (Figure 1c,d). Namibia's growing season overlaps with the rainy season, which starts in September and ends in April of the next year.

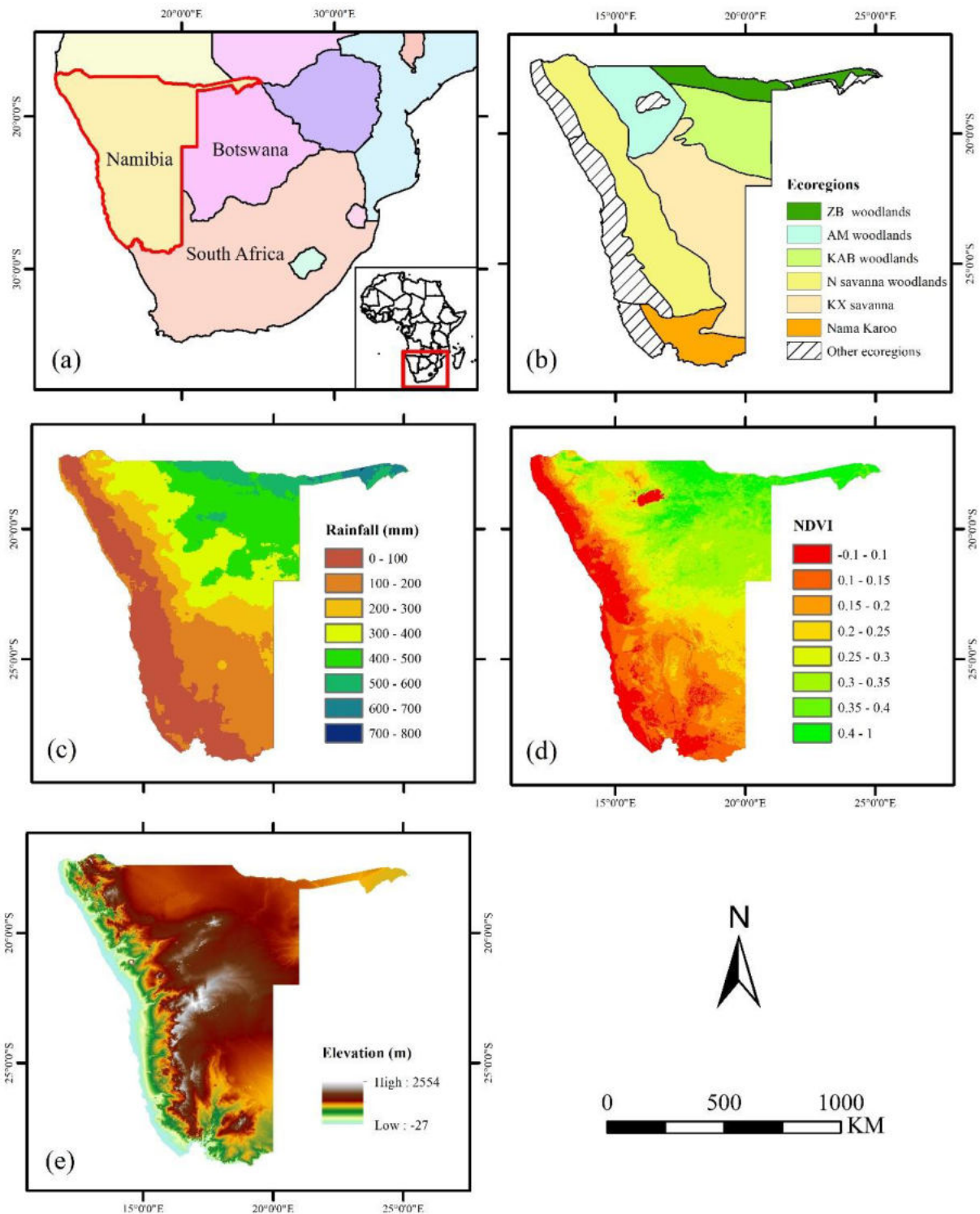


**Figure 1.** (a) Geographical location; (b) Ecological Division; (c) Average annual rainfall (2001–2020); (d) Average NDVI (2001–2020); and (e) Elevation of Namibia.



## 2.2. Data

CHIRPS (Climate Hazards Group Infrared Precipitation with Stations) was produced by the United States Geological Survey and the University of California Climate Hazards Group to provide a global precipitation dataset across 50° S–50° N from 1981 to the present [42]. The scarcity of meteorological stations in remote areas, outdated instruments and equipment, low data accuracy, and discontinuous observation data make it difficult to conduct consistent drought monitoring and assessment [29]. The rainfall estimates in the CHIRPS dataset are derived by combining satellite rainfall estimates with in situ rain gauge observations, which can provide a complete, reliable, and up-to-date dataset for seasonal drought monitoring or climate trend analysis, particularly critical in areas where station data are scarce [43]. The CHIRPS product has been widely applied in drought monitoring and evaluation across the world, especially in Africa; most studies reveal the powerful performance of this product for capturing large-scale rainfall dynamics [44–47]. This study used CHIRPS-v2.0 precipitation data ranging from 1981 to 2020, with a temporal resolution of 5 days and a spatial resolution of 0.05° (~5 km).

The MODIS sensor onboard the TERRA satellite (launched by NASA in 2000) is capable of acquiring multispectral observations of the land surface with global coverage once a day, which in turn provides global vegetation index products for nearly 20 years [48]. The NDVI layer of the MOD13A2 product for the period 2001–2020 was selected for vegetation anomaly detection. The product has a temporal resolution of 16 days and a spatial resolution of 1 km.

The Terrestrial Ecoregions of the World dataset, published by the World Wildlife Fund International (WWF), is a biogeographical regionalization of the Earth's terrestrial biodiversity [49]. The biogeographic units are ecoregions, which are defined as relatively large units of land or water containing a distinct assemblage of natural communities sharing a large majority of species, dynamics, and environmental conditions. TEOW differentiates 867 terrestrial ecoregions, classified into 14 Major Habitat Types such as forests, grasslands, or deserts. Namibia contains six main ecoregions in addition to desert areas, namely Zambezian Baikiaea woodlands (ZB woodlands), Kalahari Acacia–Baikiaea woodlands (KAB woodlands), Angolan Mopane woodlands (AM woodlands), Kalahari xeric savanna (KX savanna), Namibian savanna woodlands (N savanna woodlands), and Nama Karoo (Figure 1b).

## 2.3. Methods

In order to evaluate the continuous drought events comprehensively, the analysis of the study was mainly conducted in three parts. Firstly, the long-term trend in both rainfall forcing and vegetation response was tested using Mann–Kendall trend test [50,51], and the general coupling strength between rainfall and vegetation was quantified using correlation analysis. Next, the spatiotemporal dynamics of the three drought events were mapped using rainfall and NDVI-based drought indicators. Finally, the rainfall–vegetation interaction patterns during drought periods across landscapes were analyzed in detail in order to highlight the impact of long-term drought on ecosystem recovery. The main methods used the study are further detailed as follows.

### 2.3.1. Mann–Kendall Trend Test

The Mann–Kendall test is a nonparametric statistical test; the sample data need not be characterized by a normal distribution, and the results are not confounded by a few outliers. It is easy to calculate and is suitable for trend testing of non-normally distributed hydro-meteorological data [50–52]. For a time series  $x(x_1, x_2, \dots, x_n)$  of length  $n$ , the Mann–Kendall test statistic  $S$  is defined as:

$$S = \sum_{i=1}^{n-1} \sum_{j=i+1}^n \text{sgn}(x_j - x_i) \quad (1)$$

where  $n$  is the length of the time series,  $x_j$  and  $x_i$  are the variables of the  $j$ -th and  $i$ -th time series ( $j > i$ ), and  $sgn(x_j - x_i)$  is a symbolic function; the calculation formula can be presented as follows:

$$sgn(x_j - x_i) = \begin{cases} 1, & x_j - x_i > 0 \\ 0, & x_j - x_i = 0 \\ -1, & x_j - x_i < 0 \end{cases} \tag{2}$$

When  $n \geq 10$ , the statistic  $S$  roughly follows a normal distribution with a mean of 0. The variance of the statistic  $S$  is calculated as follows:

$$Var(S) = \frac{n(n-1)(2n+5) - \sum_{k=1}^m t_k(t_k-1)(2t_k+5)}{18} \tag{3}$$

where  $t_k$  is the number of data points in the  $k$ -th group. The change in time series trend is judged by the standard normal distribution statistic  $Z_c$ , and the constructive test statistic  $Z_c$  is calculated as follows:

$$Z_c = \begin{cases} \frac{S-1}{\sqrt{Var(S)}}, & S > 0 \\ 0, & S = 0 \\ \frac{S+1}{\sqrt{Var(S)}}, & S < 0 \end{cases} \tag{4}$$

Test the null hypothesis  $H_0$  (no monotonic trend) compared to the alternative hypothesis  $H_\alpha$  (monotonic increasing trend), and reject the null hypothesis  $H_0$  and accept the alternative hypothesis  $H_\alpha$  if  $|Z_c| \geq Z_{1-\alpha/2}$  at a given  $\alpha$  confidence level. Thus, there is a significant uptrend or downtrend in the time series at the given confidence level. A positive value of the statistic  $Z_c$  indicates that the series shows an uptrend, and a negative value of the statistic  $Z_c$  indicates that the series shows a downtrend.

### 2.3.2. Calculation of SPI

SPI is a meteorological drought index defined based on long time series precipitation which describes the variability of precipitation according to the probability of Gamma distribution. Precipitation with a skewed probability distribution is normalized [53]. The calculation steps of SPI can be presented as follows:

(1) Assuming that the precipitation at a certain period is a random variable  $x$ , the probability density function of  $\Gamma$  distribution is as in Equation (5):

$$f(x) = \frac{1}{\beta^\gamma \Gamma(\gamma)} x^{\gamma-1} e^{-x/\beta}, \quad x > 0 \tag{5}$$

where  $\gamma$  and  $\beta$  are the shape and scale parameters, respectively, which can be obtained by using the maximum likelihood estimation method as in Equations (6) and (7).

$$\hat{\gamma} = \frac{1 + \sqrt{1 + 4A/3}}{4A} \tag{6}$$

$$\hat{\beta} = \bar{x} / \hat{\gamma} \tag{7}$$

$A = \lg \bar{x} - \frac{1}{n} \sum_{i=1}^n \lg x_i$ , where  $x_i$  is the precipitation sample and  $\bar{x}$  is the average precipitation.

After determining the parameters in the probability density function, for a year of precipitation  $x_0$ , the probability of an event where the random variable  $x$  is less than  $x_0$  can be calculated, and the approximate estimate of the probability of the event can be obtained by using numerical integration after substituting Equation (5) into Equation (8).

$$F(x < x_0) = \int_x^{x_0} f(x) dx \tag{8}$$

(2) The probability of the event when precipitation is 0 can be estimated from Equation (9):

$$F(x = 0) = m/n \quad (9)$$

where  $m$  is the number of samples with zero precipitation and  $n$  is the total number of samples.

(3) The probabilities of the distribution of  $\Gamma$  are normalized by substituting the probability values obtained from Equations (8) and (9) into the normalized normal distribution function.

$$F(x < x_0) = \frac{1}{\sqrt{2\pi}} \int_x^{x_0} e^{-Z^2/2} dx \quad (10)$$

An approximate solution of Equation (10) yields the value of  $Z$  (SPI):

$$Z = S \left\{ t - \frac{(c_2 t + c_1)t + c_0}{[(d_3 t + d_2)t + d_1]t + 1.0} \right\} \quad (11)$$

$t = \sqrt{\ln \frac{1}{F^2}}$ , where  $F$  is the probability of precipitation distribution associated with the  $\Gamma$  function,  $x$  is the precipitation sample, and  $S$  is the positive and negative coefficients of probability density. When  $F > 0.5$ ,  $S = 1$ ; when  $F \leq 0.5$ ,  $S = -1$ . The calculated parameters are  $c_0 = 2.515517$ ,  $c_1 = 0.802853$ ,  $c_2 = 0.010328$ ,  $d_1 = 1.432788$ ,  $d_2 = 0.189269$ ,  $d_3 = 0.001308$ .

SPI is widely utilized in drought monitoring because it can characterize drought dynamics on multiple time scales. It has been recommended by the World Meteorological Organization (WMO) as an index for monitoring meteorological drought. SPI can measure rainfall deficit across a range of timescales. Shorter timescale SPI (e.g., three-month SPI) can provide early warning of drought. In this study, CHIRPS precipitation data (CHIRPS Pentad-Version 2.0) with a resolution of 5km archived on the GEE platform was used to calculate three-month SPI over Namibia during drought periods.

### 2.3.3. Calculation of SVI

The Standardized Vegetation Index (SVI) is calculated by standardizing the difference between the current NDVI and the long-term average NDVI of the same period. The calculation formula can be presented as follows:

$$SVI_i = \frac{NDVI_{ij} - \overline{NDVI}_i}{\sigma_i} \quad (12)$$

where  $NDVI_{ij}$  is the NDVI value of the  $i$ -th month in the  $j$ -th year,  $\overline{NDVI}_i$  is the mean NDVI value of the  $i$ -th month in many years, and  $\sigma_i$  is the standard deviation of NDVI of the  $i$ -th month in many years.

The SVI index reflects the extent to which NDVI deviates from normal values (i.e., historical mean values), which can be used as an indicator of vegetation status response to rainfall variation over water-limited ecosystem such as Namibia. The 16-day NDVI was first aggregated to monthly scale, then the SVI was calculated. As a scandalized indicator, the SVI shares the same value range as SPI.

## 3. Results

### 3.1. Climate and Ecological Conditions in Namibia

#### 3.1.1. Inter-Annual Variations of Precipitation and NDVI from 2001 to 2020

Between 2001 and 2020, Namibia experienced obvious uptrends in both cumulative precipitation and cumulative NDVI in the first ten years (from 2001 to 2010), while the cumulative precipitation and cumulative NDVI show a downtrend in the second decade (from 2011 to 2020) (Figure 2). In addition, the intensity (absolute slope of the linear regression line) of the downtrend of the second decade is much stronger than that of the uptrend in the first decade. The extremely low cumulative precipitation and cumulative

NDVI in 2013, 2015–2016 and 2019, respectively, indicate that severe meteorological drought occurred in these years, which had significant impacts on regional ecosystems.

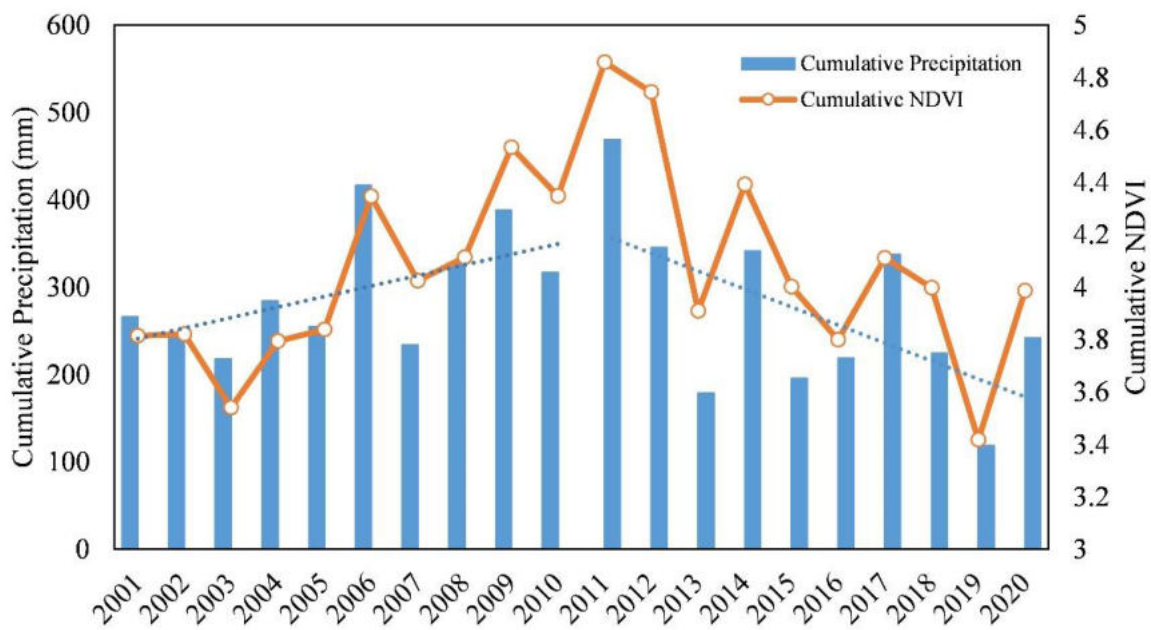


**Figure 2.** Inter-annual variation of cumulative precipitation and cumulative NDVI during the growing season (September to the following April) in Namibia between 2001 and 2020.

In order to analyze the spatial pattern of the NDVI trends in Namibia over the last 20 years, this study calculated the slope (Sen’s slope) of NDVI in Namibia for 2001–2010 and 2011–2020 using the Mann–Kendall trend test method. Pixels passing the significance trend test with a confidence level of 95% are shown in Figure 3. In the first decade, only northeastern Namibia showed a significant increasing trend (Figure 3a), while the pixels showing a significant decreasing trend in NDVI were mainly spread over a large area of western and southern Namibia in the second decade (Figure 3b). The persistent extreme drought events in the last decade may have caused more serious impacts on the ecosystems in the arid and semi-arid area of the country.

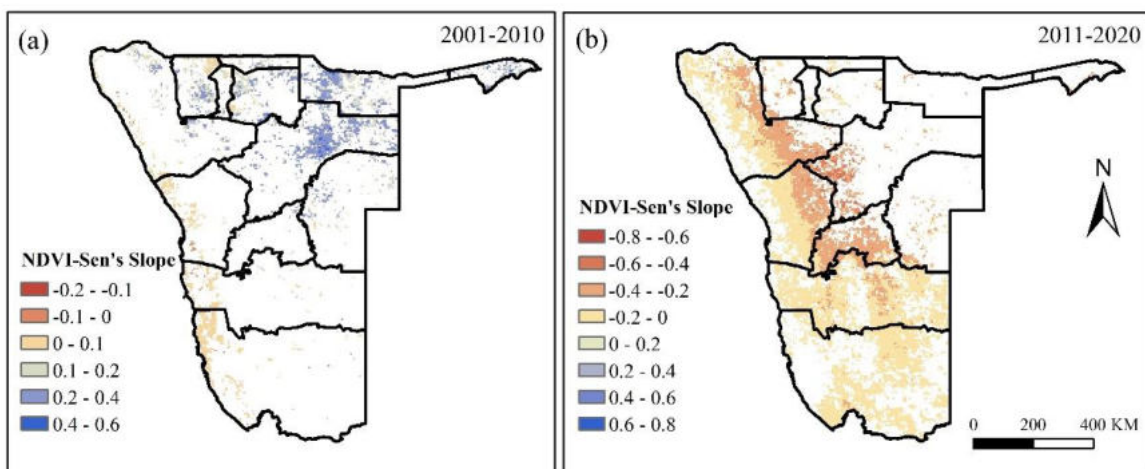


**Figure 3.** Spatial variation trends in cumulative NDVI during the growing season in Namibia for (a) 2001–2010 and (b) 2011–2020. Areas without significant trends are shown in white.



### 3.1.2. Correlation Analysis of Precipitation and NDVI in Namibia

In arid and semi-arid zones, precipitation is the main limiting factor for vegetation growth. The correlation between precipitation and vegetation indicates the coupling strength between meteorological drought and agricultural drought, i.e., high correlation between precipitation and vegetation implies that abnormal precipitation (negatively in drought) may propagate vegetation in a dynamic process with high probability, and vice versa. To investigate the relationship between precipitation and NDVI, this study analyzed the correlation between cumulative precipitation and cumulative NDVI over the last 20 years across six ecoregions of Namibia. Thus, a “spatial model” of the vegetation–precipitation relationship was constructed in this paper [54].

Considering all ecoregions, significant correlation between precipitation and NDVI in the same season ( $r = 0.90$ ,  $p < 0.01$ ) and between precipitation in the current season and cumulative NDVI in the next season ( $r = 0.87$ ,  $p < 0.01$ ) can be seen in Figure 4a,b, respectively. This indicates that vegetation productivity in the region benefits from the water supplied by both the current and previous rainy seasons. Further, by separating all rainy seasons into “wet” and “dry” seasons according to seasonal total precipitation, the difference in the relationship between cumulative precipitation and next-season cumulative NDVI was investigated. When the current season was a wet year, the correlation between the current season’s accumulated precipitation and the next season’s accumulated NDVI is relatively strong (the current season is a wet year:  $r = 0.96$ ,  $p < 0.01$ ; the current season is a continuous wet year:  $r = 0.95$ ,  $p < 0.01$ ) (Figure 4c,e). Due to heavy precipitation in the current season, water is conserved in the soil for re-use by the next year’s vegetation. On the contrary, when the season is a dry year the correlation between the current season’s accumulated precipitation and the next season’s accumulated NDVI is relatively weak (the current season is a dry year:  $r = 0.96$ ,  $p < 0.01$ ; the current season is a continuous dry year:  $r = 0.95$ ,  $p < 0.01$ ) (Figure 4d,f). This indicates that the contribution of the current season’s precipitation to the next year’s vegetation will be reduced accordingly.

For individual ecoregions, the vegetation–precipitation relationship is expressed as a “temporal model” [55]. The “temporal model” relationship shows a smaller slope compared to the “spatial model”. This indicates that the effect of temporal precipitation variation on vegetation is much smaller than that of spatial precipitation variation. For the dry year case, the slope of the “temporal model” relationship for each ecoregion was close to 0 (Figure 4d), which further indicates that precipitation in dry years has limited influence on vegetation growth in the next season.

### 3.2. Spatiotemporal Evolution of Continuous Drought in Namibia

Based on the long term precipitation and vegetation index datasets, this study calculated three-month scale SPI and one-month scale SVI for tracking the dynamic evolution of the three drought events in Namibia in 2013, 2015–2016, and 2019.

In 2013, serious drought hit most of the country, especially the northern and eastern parts between March and May (Figures 5a and 6a). In 2015–2016, Namibia was affected by persistent drought events for two consecutive years. The northern region was most severely affected by the drought in March 2015, and the drought-affected areas from October to December were mainly concentrated in the eastern and northern regions. The impact of the drought in 2016 extended westward and southward, while the drought was somewhat mitigated in parts of the eastern and northern regions (Figure 5b,c and Figure 6b,c). In 2019, most regions of Namibia experienced extreme drought between February and May, which was much stronger than the other two drought events in terms of spatial extent, intensity and duration (Figures 5d and 6d).

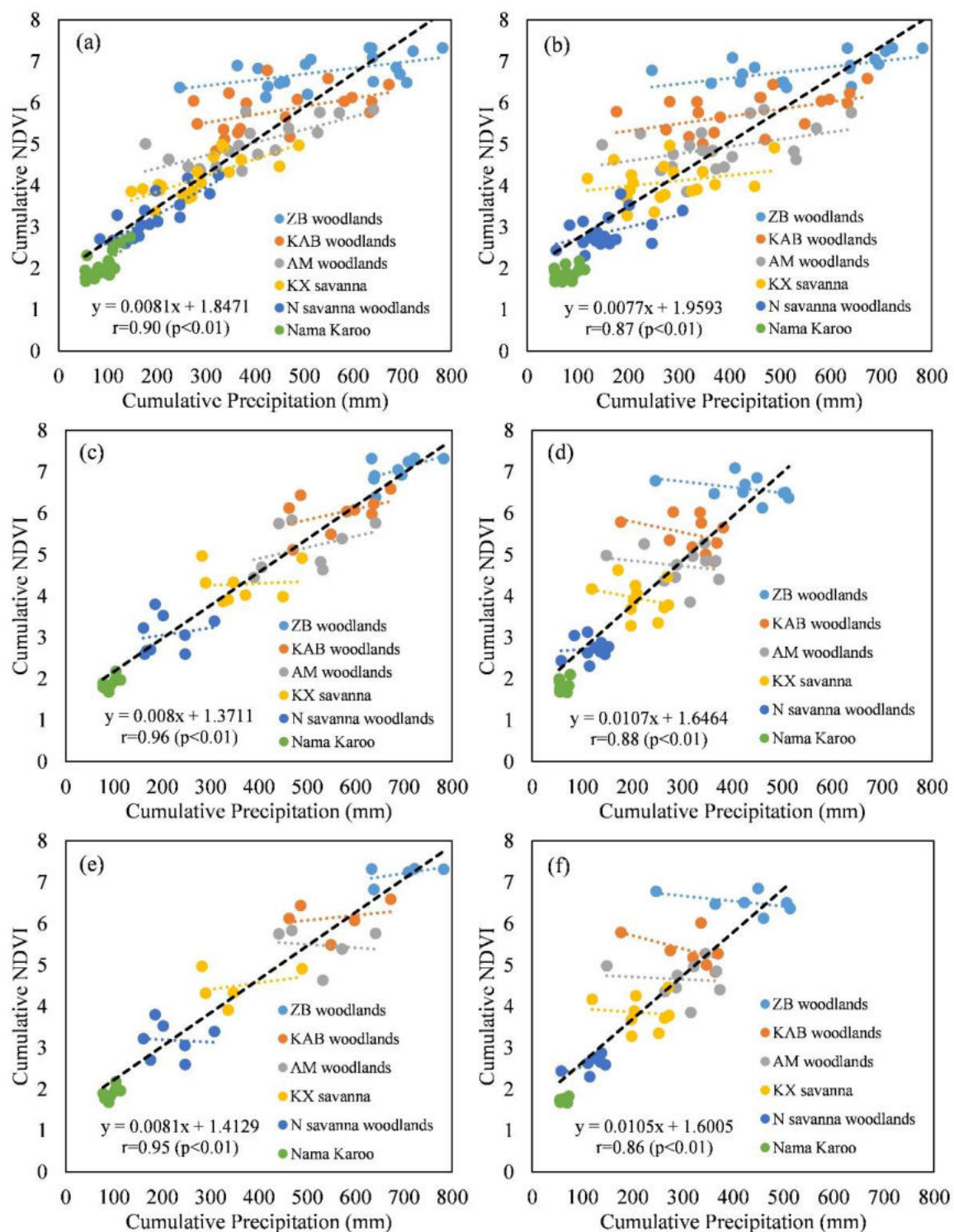


**Figure 4.** Scatterplot of seasonal cumulative precipitation and cumulative NDVI in Namibia over the past 20 years: (a) Cumulative precipitation in the current season vs. cumulative NDVI in the current season; (b) Cumulative precipitation in the current season vs. cumulative NDVI in the following season; (c) Cumulative precipitation in the current season vs. cumulative NDVI in the following season in wet years; (d) Cumulative precipitation in the current season vs. cumulative NDVI in the following season in dry years; (e) Cumulative precipitation in the current season vs. cumulative NDVI in the following season in consecutive wet years; (f) Cumulative precipitation in the current season vs. cumulative NDVI in the following season in consecutive dry years. The cumulative precipitation/NDVI in the current season represents the sum of precipitation/NDVI during the growing season.

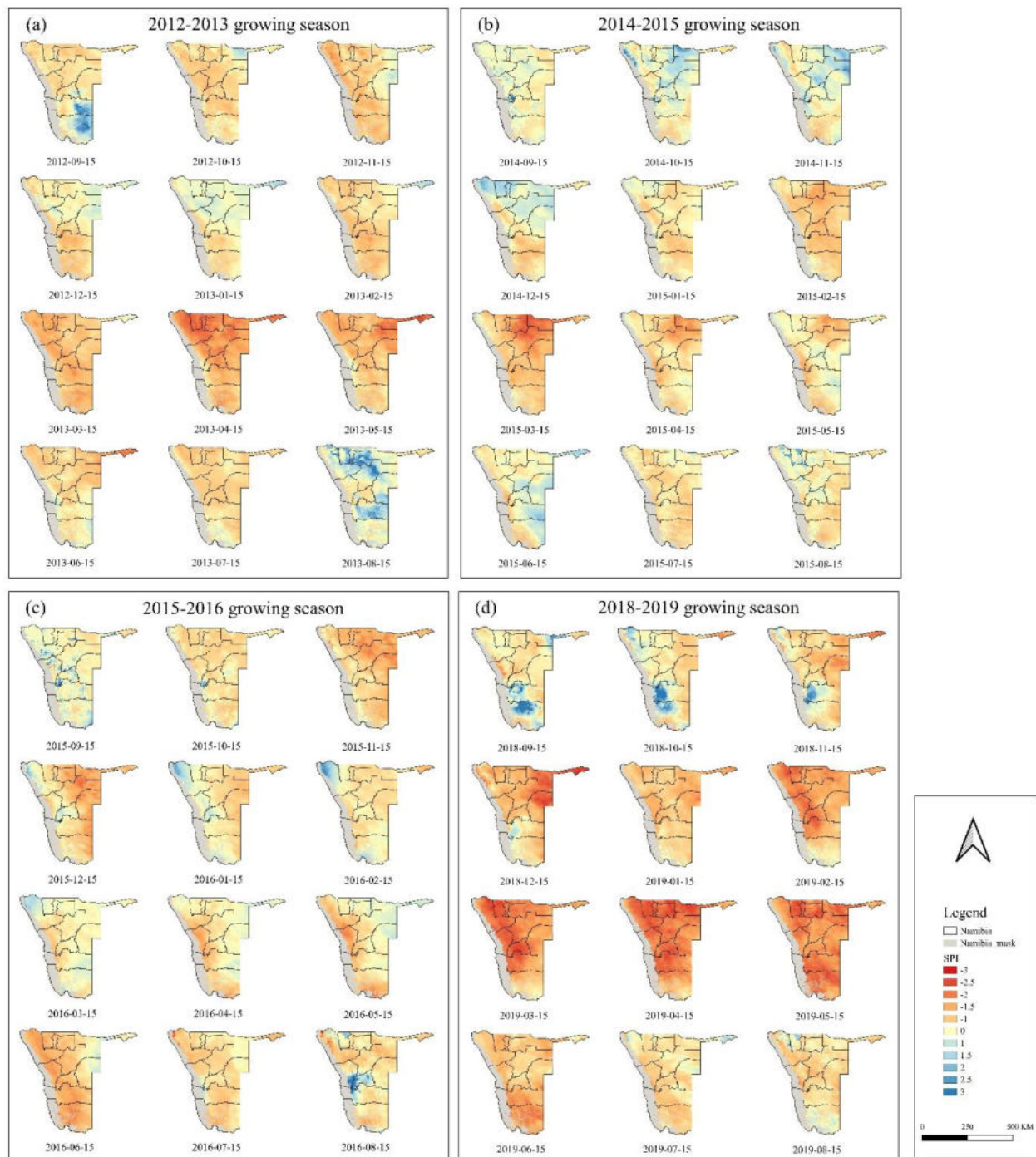


**Figure 5.** Spatiotemporal dynamics of SPI (three-month): (a) SPI in the 2012–2013 growing season; (b) SPI in the 2014–2015 growing season; (c) SPI in the 2015–2016 growing season; (d) SPI in the 2018–2019 growing season.

To quantify the extent of the drought affected areas, the two drought monitoring indices, SPI and SVI, were classified into drought grades according to Table 1 [30]. In general, the area affected by meteorological drought characterized by SPI was larger than the area affected by ecosystem drought characterized by SVI; however, they share similar temporal dynamic characteristics. The early stage of the 2012–2013 growing season was affected by drought to a lesser extent, with most of the regions being in mild drought; drought severity gradually intensified in the middle of the growing season (March–May 2013), with an area of 700,000 km<sup>2</sup> or more in moderate drought (Figure 7a,b). Namibia was affected by persistent drought in 2015–2016, with most areas in a persistent mild drought. During the 2014–2015 growing season, meteorological drought was concentrated



in the middle of the growing season (February–April 2015), with an area of 500,000 km<sup>2</sup> above moderate drought (Figure 7c,d). During the 2015–2016 growing season, drought was concentrated in the beginning (November–December 2015) and end (April–July 2016) of the growing season (Figure 7e,f). During the 2018–2019 growing season, the entire country of Namibia was affected by drought that lasted throughout the growing season, with an area of 800,000 km<sup>2</sup> above moderate drought (Figure 7g,h).

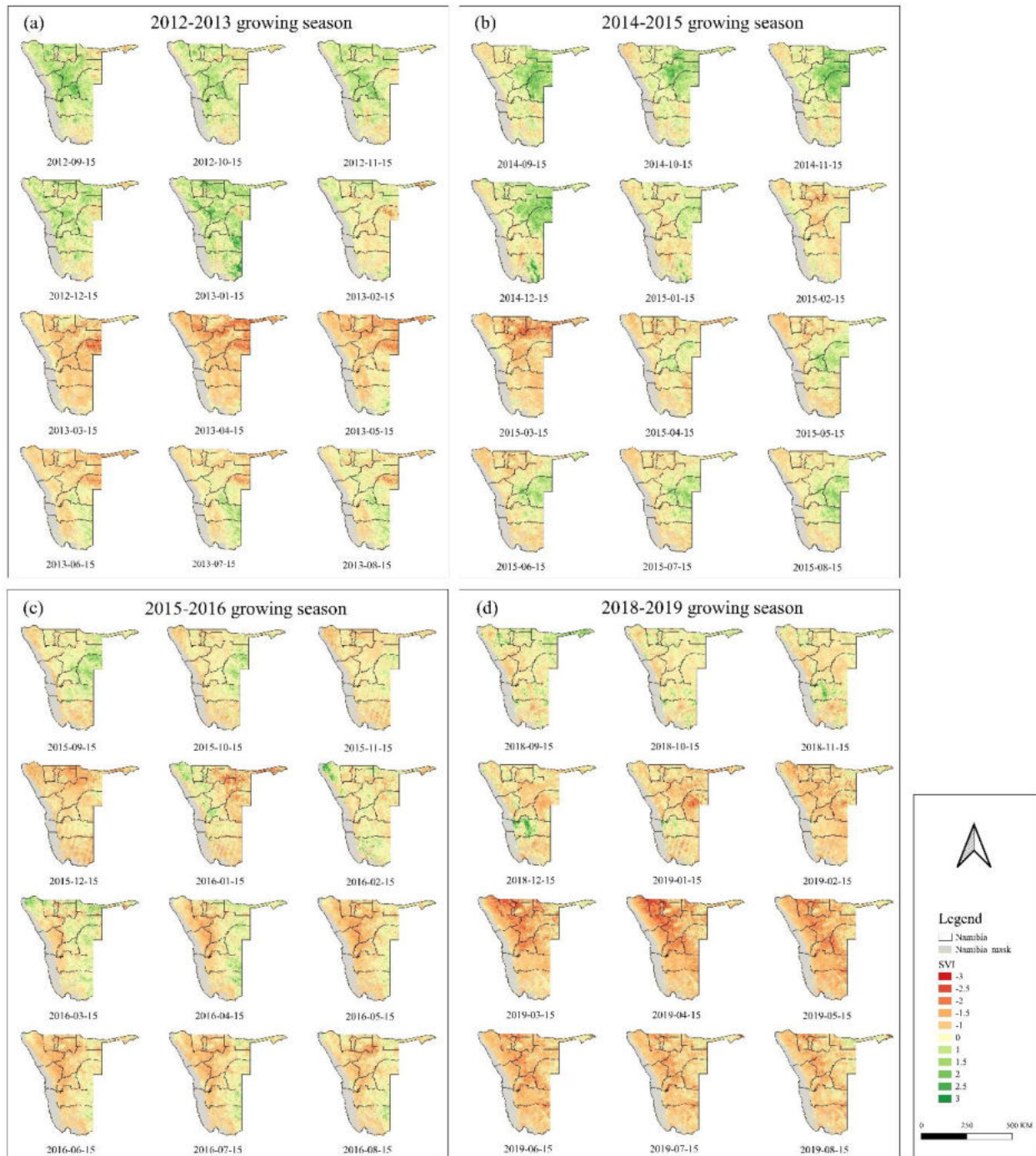


**Figure 6.** Spatiotemporal dynamics of SVI (one-month): (a) SVI in the 2012–2013 growing season; (b) SVI in the 2014–2015 growing season; (c) SVI in the 2015–2016 growing season; (d) SVI in the 2018–2019 growing season.

**Table 1.** Drought grades according to drought indices.

SPI/SVI	Drought Grades
$> -0.49$	No drought
$-0.5--0.99$	Mild drought
$-1.0--1.49$	Moderate drought
$-1.5--1.99$	Severe drought
$< -2.0$	Extreme drought

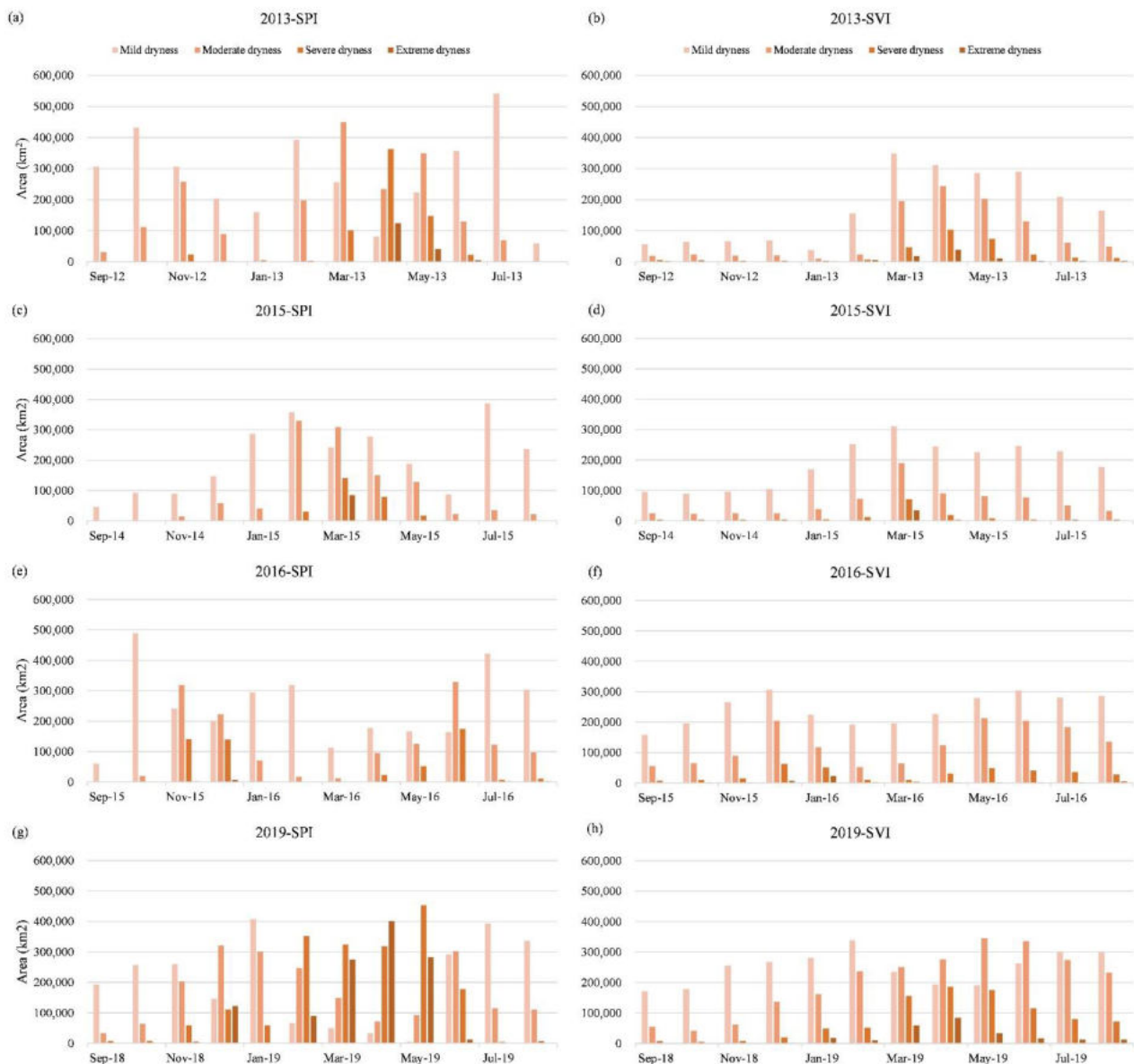


**Figure 7.** SPI/SVI drought area statistics map of three drought events in Namibia: (a) Monthly drought area evolution of SPI, 2013; (b) Monthly drought area evolution of SVI, 2013; (c) Monthly drought area evolution of SPI, 2015; (d) Monthly drought area evolution of SVI, 2015; (e) Monthly drought area evolution of SPI, 2016; (f) Monthly drought area evolution of SVI, 2016; (g) Monthly drought area evolution of SPI, 2019; (h) Monthly drought area evolution of SVI, 2019.

### 3.3. The Rainfall–Vegetation Interaction during Extreme Drought Events across Landscapes

Drought causes ecological degradation and limits the normal growth of vegetation, and thus negatively affects the ecosystem. To assess the impact of the three drought events on the ecosystem in Namibia, this study compared the variation of cumulative precipitation



and cumulative NDVI before, during, and after the three drought events in six different ecoregions (Figure 8).

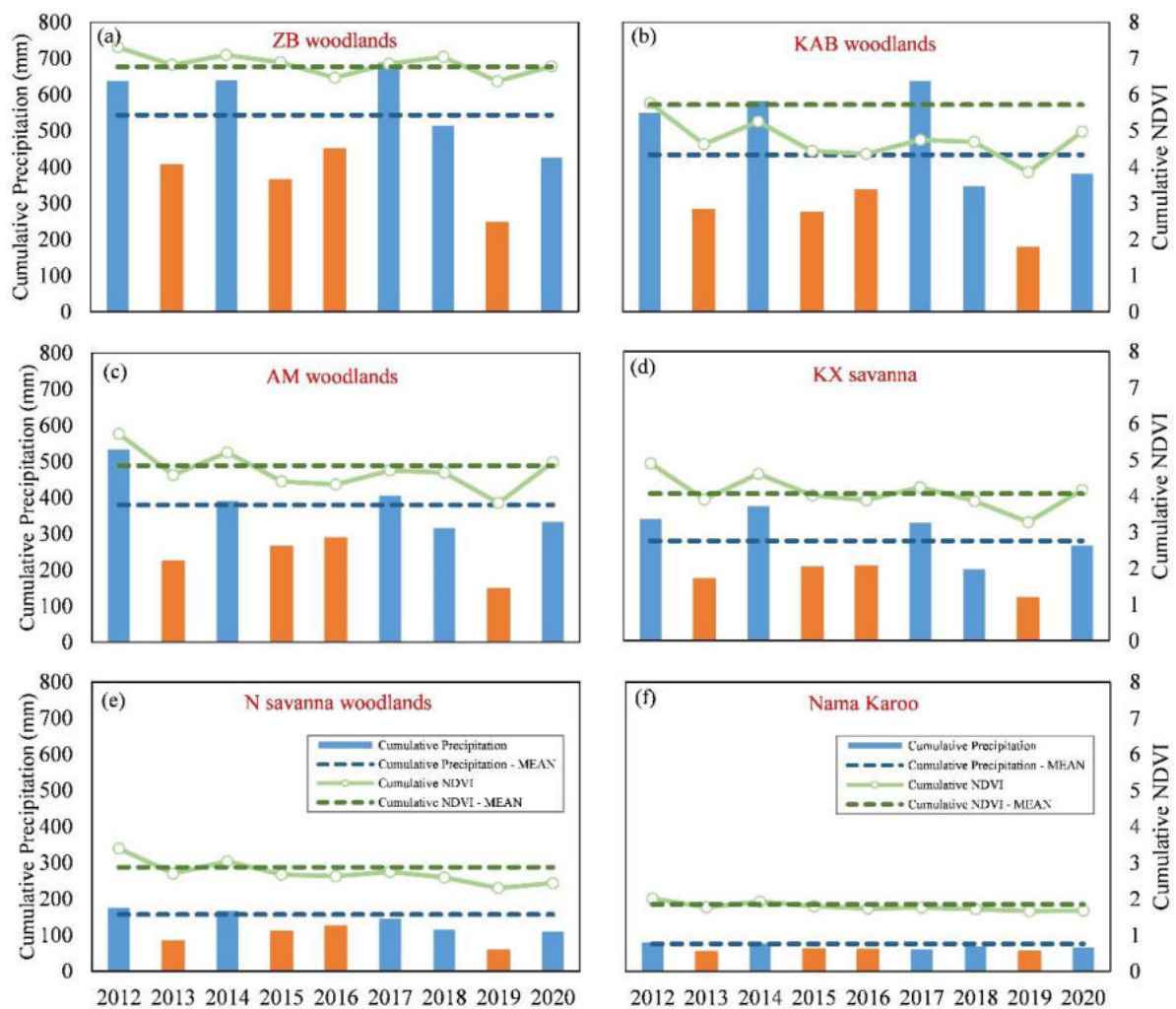


**Figure 8.** Comparative analysis of the three drought events before, during, and after drought in different ecological zones in Namibia: (a) ZB Woodlands; (b) KAB Woodlands; (c) AM Woodlands; (d) KX Savanna; (e) N Savanna Woodlands; and (f) Nama Karoo.

For both the 2013 and 2015–2016 drought events, the post-drought cumulative NDVI in all six ecoregions could not recover to the pre-drought level. Even though the post-drought cumulative precipitation was higher than the pre-drought cumulative precipitation in some ecoregions, the post-drought cumulative NDVI was still lower than the pre-drought cumulative NDVI. For example, the cumulative precipitation of KAB woodlands (Figure 8b) in 2012 and 2014 was almost the same, while after the 2013 drought event, the cumulative NDVI in 2014 (~5.2) was much lower than the cumulative NDVI in 2012 (~5.7).

The 2019 drought event was followed by a recovery in precipitation in 2020 (although still below the multi-year average), with seasonal cumulative NDVI essentially recovering to 2018 levels (or higher) which can be explained by each ecoregion already being in a drought state (with annual precipitation below the multi-year average) in 2018. In addition, with the exception for ZB woodlands, which have a relatively wetter climate, all ecoregions show a decreasing trend in cumulative NDVI since the 2013 drought event, and most are below the long-term average. These results suggest that after experiencing sustained drought events, the balance of the ecosystem may have suffered some disruption. It is likely that a return to the multi-year average state will not be obtained in the next rainy season, even with abundant rainfall.

#### 4. Discussion and Conclusions

Namibia has experienced three widespread drought events in the last decade. These continuous drought events have affected not only humans, animals (livestock and wildlife), crops, and vegetation, but also local ecosystem functions and processes. According to the news reports, the 2018/2019 drought in Namibia is the worst in 90 years, which is much more serious than the 2012/2013 drought that is reported as the worst in 30 years [18]. These reports had been confirmed by our results that the dry period captured by SVI and SPI of 2018/2019 season are more intensive in terms of both the duration and the spatial extent compared to that of the 2012/2013 season. Moreover, large amount of livestock and agriculture loss was reported for each drought event, especially the 2018/2019 event [18]. The reduction in vegetation greenness revealed by SVI map provided a clue to track the places where serious damage occurred. For example, the negative SVI across almost the whole country sustained the second half of 2018/2019 rain season (from February to May), which further explained the local impact of the drought was claimed from all sectors [17,18].

Climate projections for Namibia indicate that climate change will exacerbate changes in precipitation in the region, leading to a drier local climate, further water scarcity, lack of drinking water for both humans and animals, and reduced crop yields, which in turn will have a very serious influence on local ecosystems. The drought events of 2013, 2015–2016, and 2019 are stern warnings for the stability of Namibian ecosystem under climate change. As one of the driest countries in sub-Saharan Africa, the ecosystems, livelihoods and development of Namibia are dominated by limited rainfall, which normally presents significant inter- and intra-annual variability [56]. The intense coupling of vegetation growth to climate across the different landscapes of Namibia was confirmed by the observed strong correlation between accumulated NDVI and rainfall. Water supply shortages caused by irregular reoccurrence of drought cause unpredictable challenges for local people and livestock [17]. In this case, detailed evaluation of historical drought events and assessment of their impacts on the ecosystem is of critical importance for regional drought preparedness and drought risk reduction in the future [18]. From the perspective of the forcing-response system, rainfall is the main driving factor for an arid ecosystem, while vegetation is the direct response signal to rainfall pulses [57]. Based on the long-term rainfall and vegetation index data derived from earth observation, this study provided a synthesized evaluation of the continuous extreme drought events over the last decade characterizing not only the initial spatiotemporal dynamic of events, but also confirmed that these long-lasting water shortages may cause ecosystem degradation. Unlike previous studies of these drought events, which considered each event separately, this study investigated the three events together as a compound disaster. In this way, the stack effects of the continuous events may be more easily revealed [58,59]. In the 1970 and 1980s, the Sahel also experienced continuous drought periods for more than ten years [60], a similar situation to that of Namibia over the past decade. The damage of the Sahel drought to regional ecosystems continued for more than 30 years, and whether the ecosystem has fully recovered from that drought is still under debate [61]. In the context of future climate change scenarios, already dry areas may become drier [62]; how the drought will develop in arid Namibia over the next decade is extremely critical for local people as well as for governance policies.

In summary, the following conclusions can be derived from our results.

(1) Both the SPI and SVI drought monitoring indices were effective in capturing the dynamic evolution of drought in Namibia with spatial and temporal consistency. From March to May 2013, the drought-affected areas were mainly concentrated in the northern and eastern regions, and the northern regions were most severely affected by the drought in March 2015. The impact of the drought gradually expanded in 2016, with further expansion from the eastern and northern regions to the west and south. However, most regions of Namibia were affected by severe drought in 2019. In terms of impact area and drought intensity, the 2019 drought was the most severe, followed by 2013; the 2015–2016 drought spanned two years, but had the weakest impact.

(2) From 2001 to 2010, the growing season NDVI and precipitation in Namibia showed an overall increasing trend, and from 2011 to 2020, the growing season NDVI and precipitation showed a significant decreasing trend. Growing season NDVI was positively correlated with precipitation, and growing season NDVI was highly dependent on precipitation. There was a significant correlation ( $r = 0.90$ ,  $p < 0.01$ ) between the current season's cumulative precipitation and the current season's cumulative NDVI during the growing season in Namibia. There was also a good correlation between the current season's cumulative precipitation and the next season's cumulative NDVI ( $r = 0.87$ ,  $p < 0.01$ ). Additionally, in wet years the correlation between the current season's cumulative precipitation and the next season's cumulative NDVI was highly significant ( $r = 0.96$ ,  $p < 0.01$ ). The current season's precipitation is stored in the soil for re-use in the next season's plant growth. The effect is particularly pronounced on deep-rooted woody plants in the northern plains of Namibia.

(3) The successive extreme drought events of the last decade may have caused damage to most of Namibia's ecosystems that cannot be recovered in a short period.

**Author Contributions:** Idea, J.Z.; methodology, J.Z.; data processing, X.L.; writing—original draft preparation, X.L.; writing—review and editing, J.Z.; visualization, X.L.; supervision, J.Z. All authors have read and agreed to the published version of the manuscript.

**Funding:** This research was funded by National Key Research and Development Program of China (Grant No. 2017YFB0504105), National Natural Science Foundation of China (No. 4217011615), Fundamental Research Funds for the Central China Normal University (CCNU19TD002).

**Institutional Review Board Statement:** Not applicable.

**Informed Consent Statement:** Not applicable.

**Data Availability Statement:** Data sharing not applicable.

**Conflicts of Interest:** The authors declare no conflict of interest.

## References

1. Wilhite, D.A. *Drought as a Natural Hazard: Concepts and Definitions*; Routledge: London, UK, 2000; pp. 3–18.
2. Vogel, C.; Laing, M.; Monnik, K. Drought in South Africa, with Special Reference to the 1980–94 Period. In *Drought: A Global Assessment*; Routledge: London, UK, 2000; pp. 348–366.
3. Riebsame, W.E. *Drought and Natural Resources Management in The United States: Impacts and Implications of the 1987–89 Drought*; Rutledge: London, UK, 2019; ISBN 978-0-429-71455-9.
4. Byers, B.A. *Environmental Threats and Opportunities in Namibia: A Comprehensive Assessment*; Directorate of Environmental Affairs, Ministry of Environment and Tourism: Windhoek, Namibia, 1997.
5. Klugman, J. *Human Development Report 2011. Sustainability and Equity: A Better Future for All*; Social Science Electronic Publishing: Rochester, NY, USA, 2011; pp. 732–743.
6. Næraa, T. *Coping with Drought in Namibia: Informal Social Security Systems in Caprivi and Erongo, 1992*; NISER, Multi-Disciplinary Research Centre, University of Namibia: Windhoek, Namibia, 1993.
7. Devereux, S.; Næraa, T. Drought and Survival in Rural Namibia. *J. South. Afr. Stud.* **1996**, *22*, 421–440. [[CrossRef](#)]
8. Ashipala, S.N. Effect of Climate Variability on Pearl Millet (*Pennisetum Glaucum*) Productivity and the Applicability of Combined Drought Index for Monitoring Drought in Namibia. Master's Thesis, University of Nairobi, Nairobi, Kenya, 2013.
9. Luetkemeier, R.; Liehr, S. Integrated Responses to Drought Risk in Namibia and Angola. *Water Solut.* **2019**, *3*, 56–61.
10. President Declares Drought Emergency—Namibia. Available online: <https://reliefweb.int/report/namibia/president-declares-drought-emergency> (accessed on 4 March 2021).
11. Namibia's Devastating Drought: Our Strategy so Far—Namibia. Available online: <https://reliefweb.int/report/namibia/namibia-s-devastating-drought-our-strategy-so-far> (accessed on 4 March 2021).
12. Fara, K. How Natural Are 'Natural Disasters'? Vulnerability to Drought of Communal Farmers in Southern Namibia. *Risk Manag.* **2001**, *3*, 47–63. [[CrossRef](#)]
13. Masih, I.; Maskey, S.; Mussá, F.E.F.; Trambauer, P. A Review of Droughts on the African Continent: A Geospatial and Long-Term Perspective. *Hydrol. Earth Syst. Sci.* **2014**, *18*, 3635–3649. [[CrossRef](#)]

14. Onywere, S.; Shisanya, C.; Obando, J.; Masiga, D.; Irura, Z.; Mang, S. Geospatial Extent of 2011–2013 Flooding from the Eastern African Rift Valley Lakes in Kenya and Its Implication on the Ecosystems. The Soda Lakes of Kenya: Their Current Conservation Status and Management, Conference Report Held at Kenya Wildlife Service Training Institute–Naivasha, Kenya on. 2013. Available online: [http://ku.ac.ke/schools/environmental/images/stories/research/Geospatial\\_Extent\\_20011-2013.pdf](http://ku.ac.ke/schools/environmental/images/stories/research/Geospatial_Extent_20011-2013.pdf) (accessed on 19 October 2021).
15. Monyela, B.M. *A Two-Year Long Drought in Summer 2014/2015 and 2015/2016 over South Africa*; University of Cape Town: Cape Town, South Africa, 2017.
16. Meque, A.; Abiodun, B.J. Simulating the Link between ENSO and Summer Drought in Southern Africa Using Regional Climate Models. *Clim. Dyn.* **2015**, *44*, 1881–1900. [[CrossRef](#)]
17. Van Rensburg, P.; Tortajada, C. An Assessment of the 2015–2017 Drought in Windhoek. *Front. Clim.* **2021**, *3*. [[CrossRef](#)]
18. Shikangalah, R.N. The 2019 Drought in Namibia: An Overview. *J. Namib. Stud. Hist. Politics Cult.* **2020**, *27*, 37–58.
19. As Climate Shocks Intensify, UN Food Agencies Urge More Support for Southern Africa’s Hungry People | World Food Programme. Available online: <https://www.wfp.org/news/climate-shocks-intensify-un-food-agencies-urge-more-support-southern-africas-hungry-people> (accessed on 4 October 2021).
20. Dai, A. Drought under Global Warming: A Review. *WIREs Clim. Chang.* **2011**, *2*, 45–65. [[CrossRef](#)]
21. Dai, A.; Trenberth, K.E.; Qian, T. A Global Dataset of Palmer Drought Severity Index for 1870–2002: Relationship with Soil Moisture and Effects of Surface Warming. *J. Hydrometeorol.* **2004**, *5*, 1117–1130. [[CrossRef](#)]
22. Bestelmeyer, B.T.; Okin, G.S.; Duniway, M.C.; Archer, S.R.; Sayre, N.F.; Williamson, J.C.; Herrick, J.E. Desertification, Land Use, and the Transformation of Global Drylands. *Front. Ecol. Environ.* **2015**, *13*, 28–36. [[CrossRef](#)]
23. van der Molen, M.K.; Dolman, A.J.; Ciais, P.; Eglin, T.; Gobron, N.; Law, B.E.; Meir, P.; Peters, W.; Phillips, O.L.; Reichstein, M.; et al. Drought and Ecosystem Carbon Cycling. *Agric. For. Meteorol.* **2011**, *151*, 765–773. [[CrossRef](#)]
24. Henckel, P.A. Physiology of Plants Under Drought. *Annu. Rev. Plant Physiol.* **1964**, *15*, 363–386. [[CrossRef](#)]
25. Panagoulia, D.; Dimou, G. Sensitivity of Flood Events to Global Climate Change. *J. Hydrol.* **1997**, *191*, 208–222. [[CrossRef](#)]
26. Panagoulia, D. From Low-Flows to Floods under Global Warming. *EGU Gen. Assem. Conf. Abstr.* **2009**, *11*, 4511.
27. Mortimore, M. Adapting to Drought in the Sahel: Lessons for Climate Change. *WIREs Clim. Chang.* **2010**, *1*, 134–143. [[CrossRef](#)]
28. Heumann, B.W.; Seaquist, J.W.; Eklundh, L.; Jönsson, P. AVHRR Derived Phenological Change in the Sahel and Soudan, Africa, 1982–2005. *Remote Sens. Environ.* **2007**, *108*, 385–392. [[CrossRef](#)]
29. Palmer, W.C. *Meteorological Drought*; U.S. Department of Commerce, Weather Bureau: Washington, DC, USA, 1965.
30. McKee, T.; Doesken, N.; Kleist, J. The Relationship of Drought Frequency and Duration to Time Scales. In Proceedings of the 8th Conference on Applied Climatology, Anaheim, CA, USA, 17–22 January 1993; Volume 17, pp. 179–183.
31. McKee, T. Drought Monitoring with Multiple Time Scales. In Proceedings of the 9th Conference on Applied Climatology, Dallas, TX, USA, 15–20 January 1995.
32. Vicente-Serrano, S.; Beguería, S.; López-Moreno, J.I. A Multiscalar Drought Index Sensitive to Global Warming: The Standardized Precipitation Evapotranspiration Index. *J. Clim.* **2010**, *23*, 1696–1718. [[CrossRef](#)]
33. Smith, W.K.; Dannenberg, M.P.; Yan, D.; Herrmann, S.; Barnes, M.L.; Barron-Gafford, G.A.; Biederman, J.A.; Ferrenberg, S.; Fox, A.M.; Hudson, A.; et al. Remote Sensing of Dryland Ecosystem Structure and Function: Progress, Challenges, and Opportunities. *Remote Sens. Environ.* **2019**, *233*, 111401. [[CrossRef](#)]
34. Kim, Y. Drought and Elevation Effects on MODIS Vegetation Indices in Northern Arizona Ecosystems. *Int. J. Remote Sens.* **2013**, *34*, 4889–4899. [[CrossRef](#)]
35. Reddy, G.P.O.; Kumar, N.; Sahu, N.; Srivastava, R.; Singh, S.K.; Naidu, L.G.K.; Chary, G.R.; Biradar, C.M.; Gumma, M.K.; Reddy, B.S.; et al. Assessment of Spatio-Temporal Vegetation Dynamics in Tropical Arid Ecosystem of India Using MODIS Time-Series Vegetation Indices. *Arab. J. Geosci.* **2020**, *13*, 704. [[CrossRef](#)]
36. Scott, R.L.; Huxman, T.E.; Barron-Gafford, G.A.; Jenerette, G.D.; Young, J.M.; Hamerlynck, E.P. When Vegetation Change Alters Ecosystem Water Availability. *Glob. Chang. Biol.* **2014**, *20*, 2198–2210. [[CrossRef](#)] [[PubMed](#)]
37. Huang, J.; Ji, M.; Xie, Y.; Wang, S.; He, Y.; Ran, J. Global Semi-Arid Climate Change over Last 60 Years. *Clim. Dyn.* **2016**, *46*, 1131–1150. [[CrossRef](#)]
38. Rutherford, M.C. Annual Plant Production-Precipitation Relations in Arid and Semi-Arid Regions. *S. Afr. J. Sci.* **1965**, *61*, 53–56.
39. Wang, L.; D’Odorico, P. The Limits of Water Pumps. *Science* **2008**, *321*, 36–37. [[CrossRef](#)]
40. Huang, J.; Yu, H.; Guan, X.; Wang, G.; Guo, R. Accelerated Dryland Expansion under Climate Change. *Nat. Clim. Chang.* **2016**, *6*, 166–171. [[CrossRef](#)]
41. Sun, Y.; Solomon, S.; Dai, A.; Portmann, R.W. How Often Does It Rain? *J. Clim.* **2006**, *19*, 916–934. [[CrossRef](#)]
42. Funk, C.; Peterson, P.; Landsfeld, M.; Pedreros, D.; Verdin, J.; Shukla, S.; Husak, G.; Rowland, J.; Harrison, L.; Hoell, A.; et al. The Climate Hazards Infrared Precipitation with Stations—A New Environmental Record for Monitoring Extremes. *Sci. Data* **2015**, *2*, 150066. [[CrossRef](#)]
43. Funk, C.C.; Peterson, P.J.; Landsfeld, M.F.; Pedreros, D.H.; Verdin, J.P.; Rowland, J.D.; Romero, B.E.; Husak, G.J.; Michaelsen, J.C.; Verdin, A.P. A Quasi-Global Precipitation Time Series for Drought Monitoring. *US Geol. Surv. Data Ser.* **2014**, *832*, 4.
44. Toté, C.; Patricio, D.; Boogaard, H.; Van der Wijngaart, R.; Tarnavsky, E.; Funk, C. Evaluation of Satellite Rainfall Estimates for Drought and Flood Monitoring in Mozambique. *Remote Sens.* **2015**, *7*, 1758–1776. [[CrossRef](#)]



45. Dinku, T.; Funk, C.; Peterson, P.; Maidment, R.; Tadesse, T.; Gadain, H.; Ceccato, P. Validation of the CHIRPS Satellite Rainfall Estimates over Eastern Africa. *Q. J. R. Meteorol. Soc.* **2018**, *144*, 292–312. [[CrossRef](#)]
46. Muthoni, F.K.; Odongo, V.O.; Ochieng, J.; Mugalavai, E.M.; Mourice, S.K.; Hoesche-Zeledon, I.; Mwila, M.; Bekunda, M. Long-Term Spatial-Temporal Trends and Variability of Rainfall over Eastern and Southern Africa. *Theor. Appl. Climatol.* **2019**, *137*, 1869–1882. [[CrossRef](#)]
47. Obahoundje, S.; Bi, V.H.N.; Kouassi, K.L.; Ta, M.Y.; Amoussou, E.; Diedhiou, A. Validation of Three Satellite Precipitation Products in Two South-Western African Watersheds: Bandama (Ivory Coast) and Mono (Togo). *Atmos. Clim. Sci.* **2020**, *10*, 597–613. [[CrossRef](#)]
48. LP DAAC—MOD13A2. Available online: <https://lpdaac.usgs.gov/products/mod13a2v006/> (accessed on 4 March 2021).
49. Olson, D.; Dinerstein, E.; Wikramanayake, E.; Burgess, N.; Powell, G.; Underwood, E.; D’amico, J.; Itoua, I.; Strand, H.; Morrison, J.; et al. Terrestrial Ecoregions of the World: A New Map of Life on Earth. *BioScience* **2001**, *51*, 933–938. [[CrossRef](#)]
50. Mann, H.B. Nonparametric Tests Against Trend. *Econometrica* **1945**, *13*, 245–259. [[CrossRef](#)]
51. Kendall, M.G. *Rank Correlation Methods*; Griffin: Oxford, UK, 1975.
52. Gilbert, R.O. *Statistical Methods for Environmental Pollution Monitoring*; Wiley: New York, NY, USA, 1987.
53. Cheval, S. The Standardized Precipitation Index—An Overview. *Rom. J. Meteorol.* **2015**, *12*, 17–64.
54. Guo, T.; Tan, Q.; Xiong, J. Analysis of Spatial Patterns in a Vegetation Model. *Appl. Math. Comput.* **2011**, *217*, 8303–8310. [[CrossRef](#)]
55. Fang, J.; Piao, S.; Zhou, L.; He, J.; Wei, F.; Myneni, R.B.; Tucker, C.J.; Tan, K. Precipitation Patterns Alter Growth of Temperate Vegetation. *Geophys. Res. Lett.* **2005**, *32*. [[CrossRef](#)]
56. Nakanyete, N.; Shikangalah, R.N.; Vatuva, A. Drought as a Disaster in the Namibian Context. *Int. J. Sci. Res.* **2020**, *9*, 377–386. [[CrossRef](#)]
57. Zhou, J.; Jia, L.; Menenti, M.; van Hoek, M.; Lu, J.; Zheng, C.; Wu, H.; Yuan, X. Characterizing Vegetation Response to Rainfall at Multiple Temporal Scales in the Sahel-Sudano-Guinean Region Using Transfer Function Analysis. *Remote Sens. Environ.* **2021**, *252*, 112108. [[CrossRef](#)]
58. He, X.; Sheffield, J. Lagged Compound Occurrence of Droughts and Pluvials Globally Over the Past Seven Decades. *Geophys. Res. Lett.* **2020**, *47*, e2020GL087924. [[CrossRef](#)]
59. de Brito, M.M. Compound and Cascading Drought Impacts Do Not Happen by Chance: A Proposal to Quantify Their Relationships. *Sci. Total Environ.* **2021**, *778*, 146236. [[CrossRef](#)] [[PubMed](#)]
60. Zeng, N. Drought in the Sahel. *Science* **2003**, *302*, 999–1000. [[CrossRef](#)] [[PubMed](#)]
61. Kusserow, H. Desertification, Resilience, and Re-Greening in the African Sahel – A Matter of the Observation Period? *Earth Syst. Dyn.* **2017**, *8*, 1141–1170. [[CrossRef](#)]
62. Chou, C.; Chiang, J.C.H.; Lan, C.-W.; Chung, C.-H.; Liao, Y.-C.; Lee, C.-J. Increase in the Range between Wet and Dry Season Precipitation. *Nat. Geosci.* **2013**, *6*, 263–267. [[CrossRef](#)]